Adsorption 8: 235–248, 2002

Ethanol-Water Separation in the PSA Process

M.J. CARMO
Universidade Federal do Ceará, Departamento de Engenharia Química, Fortaleza, CE, Brazil

J.C. GUBULIN
Universidade Federal de São Carlos, Departamento de Engenharia Química, São Carlos, SP, Brazil

Abstract. An investigation was carried out on ethanol-water separation employing a PSA adsorption cycle with zeolite 3A as the adsorbent. The cycle was operated under the following operating variables: feed flow (2, 4, 6 and 8 L/h), adsorption temperature (200°C) and adsorption pressures (2, 4 and 6 bar). All experimental runs were performed under vacuum of 0.2 bar in the desorption step. The effect of these variables on the enrichment and recovery percentage of the product, on the productivity and on the total cycle time was studied, using the adsorption pressure as a parameter. The results showed that these variables significantly affect the responses of interest. We also studied the influence of such variables as: adsorption pressures, desorption pressures, flow rates and adsorption temperatures (T), on the enrichment, recovery, productivity and on the total cycle time. The data were obtained from operational cycles in a Kahle's system. The experiments were organized by a three level factorial design. The results obtained were compared with from the fitted empirical equations as well as with the corresponding surface responses and all variables showed to be influential. Last, by an optimal combination of the variables was obtained by means of the ridge analysis method and the optimized multi-response method.

Keywords: adsorption, zeolite, ethanol

Introduction

For automotive transport, liquid fuels are considered essential, and ethanol derived from sugar or starch by hydrolysis and fermentation is one of the most studied renewable alternatives. Although the use of pure ethanol as a fuel is a less attractive economic alternative at present, there is growing interest in oxygenated organics as substitutes for lead tetra-ethyl in high octane gasoline, and again ethanol is one of the options. A major problem in the use of fermentation ethanol as a fuel is the high energy cost associated to the separation of ethanol from the large excess of water (fermenter broths typically contain only 5–8% ethanol by weight). Older distillation units often consumed almost as much energy as the fuel value of the ethanol produced, and while modern units perform much better, distillation is still an energy intensive process. Dehydration by adsorption on a 3A molecular sieve has been suggested as a promising alternative to the conventional processes. The 3A sieve has the advantage that the micropores are too small to be penetrated by alcohol molecules so that water is adsorbed without competition from the liquid phase, as demonstrated in the works of Azevedo (1992), Carton et al. (1987), Teo and Ruthven (1986), and Sowerby and Crittenden (1991). Pressure swing adsorption (PSA) is a widely used process for the separation of gases. It is employed in a broad range of industrial applications including the recovery of hydrogen, the separation of oxygen from air, the separation of normal and iso-paraffins, and a variety of drying operations. These classes of separations, and others, have been reviewed recently (Cassidy and Holmes, 1984; Keller, 1983; Mersmann et al., 1984). PSA is attractive because it requires little energy input and operates on cycles of short duration. Therefore, it has high sorbent

productivity and is often capable of producing very pure product. This latter feature is the interest of the present paper.

Materials and Methods

3A zeolite was used as adsorbent in the form of spheres with mean diameter of 2.60 mm, as obtained by the Tyler/Mesh procedure. This adsorbent was characterized physically by water pycnometry. A quantitative and qualitative chemical analysis of this zeolite was done by mass spectrometry. The physical and chemical characterization of 3A zeolite can be found in the work of Carmo and Gubulin (1997), and is summarized in Table 1.

The bed was also characterized by determining some of its physical properties, which included the calculation of the porosity and of the packing density of the bed. A stainless steel vessel was used (30 cm long; 4.7 cm i.d.). Its dimensions ensured good flow distribution since the bed internal diameter is at least 10 times as much as the particle size and its length is at least 100 times as much as the particle size, as required by White (1988). Under these conditions, the bed volume may be calculated from Eq. (1).

$$V_{cs} = \frac{\pi \phi_{cs}^2 H_{cs}}{4} \tag{1}$$

To calculate the porosity of the bed, it was necessary to know the total mass of the particles that filled the bed. The process of bed filling started by placing the column in upright position and pouring the adsorbent at the top with the aid of a funnel. At the same time, moderate vibration was applied at the bottom of the column. By weight difference, it was possible to determine the mass of particles loaded into the column and the porosity was calculated from Eq. (2).

Table 1. Physical and chemical parameters of the 3A zeolite.

Parameter	Value
Real density (g/ml)	2.765
Apparent density (g/ml)	1.210
Porosity	0.560
Chemical composition (%)	Al_2O_3 (30.7); SiO_2 (32.4); K_2O (8.90); Na_2O (5.60); MgO (2.30); CaO (0.71)

Table 2. Physical properties of the bed.

ϕ_{cs}	4.7 cm
H_{cs}	30.0 cm
A_{cs}	17.34 cm^2
V_{cs}	520.22 cm^3
M_s	371.42 g
ρ_b	0.71 g/cm^3
ε_L	0.41

$$\varepsilon_L = 1 - \frac{M_s}{\rho_p V_{cs}} \tag{2}$$

Once the adsorbent mass contained in the bed and the total volume of the bed have been determined, the packing density was calculated from Eq. (3). The characterization parameters of the bed are shown in Table 2.

$$\rho_b = \frac{M_s}{V_{cs}} \tag{3}$$

The ethanol-water solution was prepared from anhydrous ethanol and distilled water at concentrations of around 95% wt ethanol with an accuracy of ± 0.005 g. In order to measure the concentration of the fluid phase, a Reichert-Jung Auto Abbé refractometer with automatic calibration was used and data reproducibility of 0.5% was obtained. The experimental setup was divided into three main parts: feed system (composed of a 7.5-liter tank, a positive displacement pump of piston type, solenoid valves, pipes and connections), central body (composed of an adsorption column and a vaporizer, together with a heating system and temperature control unit, solenoid valves VS1, VS2 and VS3) and a product collection system (composed of a fraction collector, a vacuum pump, a double-tube heat exchanger and a cooling bath). Figure 1 illustrates the experimental system.

Experimental Procedure

The tank was filled with an ethanol-water solution of known concentration (azeotropic composition). After filling this tank, the flow rate was measured by circulating the liquid from the tank, through valve VS1 and turning on the feed pump, with the valve opening properly adjusted. At this time valves VS2, VE1 and VE2 are closed and valve VS3 is open. A liquid sample of the

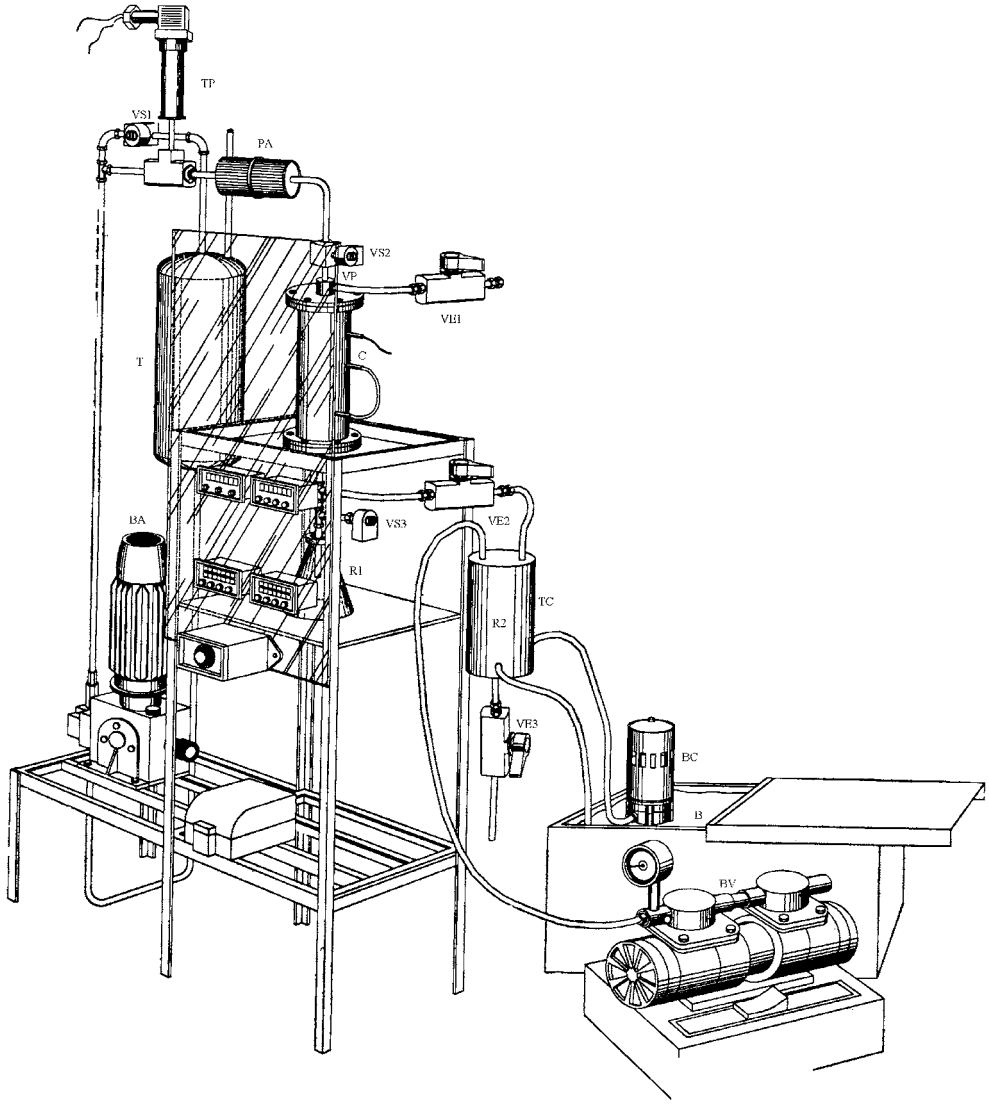

Figure 1. Adsorption plant. T, feeding reservoir; BA, feeding pump; BV, vacuum pump; BC, circulating pump; TP, pressure controller; C, adsorption bed; PA, pre-heater; R1 and R2, storing reservoirs; B, cooling bath; TC, heat exchanger; VS, solenoid valves; VE, ball valves.

feed was withdrawn with a pipette and the concentration was determined by the refractometry. After having established the feed state (defined by its flow rate and concentration), the column was packed with a mass of activated adsorbent, and the temperatures were set for the column, vaporizer and pre-heater. For all the runs the column and vaporizer were kept at the same temperature, which varied in according to a pre-established plan. The pre-heater was maintained close to the temperature of vaporization of the mixture (around 75°C). The heated parts of the plant were insulated with glass wool and the precision of the temperature controller was 0.1°C. Then, the system was pressurized (preparing for adsorption under high pressure). This pressurization was achieved by opening valve VS2 and closing valves VS1 and VS3; pressure buildup occurred due to an increase of fluid mass (vapor of ethanol-water) inside the bed. After the desired pressure was reached and the pressurization time elapsed, the system automatically opens valves VS3 and VS1 and closes valve VS2, providing vapor flow rate into reservoir R1, where it condenses, at the same time as the liquid is fed from the tank. The mass of collected product was weighed, with an accuracy of 0.001 g, and the concentration, in

ethanol wt%, were obtained by the refractometry, for each operation cycle. When the pressure reached the levels of the beginning of the pressurization, the controller closed to the valve VS3 and it opened up valve VE2, sending the fluid at a heat of double-tube heat exchanger, which was cooled with water from the bath circulation working simultaneously with the vacuum pump. The time spent in desorption stage was timed. This time is the sum of the time spent for the closing of VS2 valve and opening of VS3 valve, the time of despressurization, and the worn-out have-powder the required vacuum, for the closing of VS3 valve, opening of VE2 valve and starting of the vacuum pump, time of desorption. At the end of this cycle, the next cycle begins with the same experimental procedure. Concentrations and collected fluid masses are monitored as well as the number of cycles required to reach the steady-state. The bed was purged with nitrogen through valve VE1 prior to each experimental run. The values of the operating variables are shown in Table 3 (preliminary experiments).

All experiments were organized by a three level factorial design which allowed fitting of second order models from a reduced number of experimental points, accomplishing interactions among the variables and the linear and quadratic terms of each inlet variable. The values of the variables are in Table 4. The transformation of the variables was calculated through Eq. (4).

$$X_i = \frac{X_i^* - X_i^*(0)}{X_i^*(1) - X_i^*(0)} \tag{4}$$

Answers of interest (enrichment of the fluid phase, the percentage of product recovery, the productivity and

Table 3. Values of the variables for the preliminary experiments.

Run	T (°C)	P_h (bar)	v (l/h)	P_l (bar)
1	200	2	2	0.2
2	200	2	4	0.2
3	200	2	6	0.2
4	200	2	8	0.2
5	200	4	2	0.2
6	200	4	4	0.2
7	200	4	6	0.2
8	200	4	8	0.2
9	200	6	2	0.2
10	200	6	4	0.2
11	200	6	6	0.2
12	200	6	8	0.2

Table 4. Values of the variables for the experiments.

	Transformation of the variables		
Variables	−1	0	1
P_h (bar)	2	6	10
t_d (bar)	0.2	0.5	0.8
v (l/h)	2	5	8
T (°C)	150	200	250

total time of the cycle) were obtained from Eqs. (5)–(8), respectively, all of which were calculated at steady-state.

$$E = X_f \tag{5}$$

$$R = \frac{M_f X_f}{M_o X_o} \times 100 \tag{6}$$

$$P = \frac{M_f X_f}{M_s t} \times 3600 \tag{7}$$

$$t = t_{pr} + t_d + t_v \tag{8}$$

The mass of fluid fed, at a given fixed operation pressure and temperature, was calculated according to Eq. (9).

$$M_o = \frac{v.t_{pr}.\rho_L}{3600} \tag{9}$$

An optimal combination was obtained for the variables through the ridge analysis method. This method was used to determine the maximum or minimum value of the response adjusted by the model (Y_{pred}) inside spheres of variable radius, r_i ($i = 1, 2, \ldots$), on the central point $(X_1, X_2, \ldots, X_k) = (0, 0, \ldots, 0)$ and in the experimental range. The second order models were calculated through Eq. (10) and the restriction to find the maximum or minimum value of the response was calculated through Eq. (11).

$$Y_{pred} = \beta + X'b + X'BX \tag{10}$$

$$\sum_{i=1}^{k} X_i^2 = r^2 \tag{11}$$

The values of the coordinates $(X_1, X_2, \ldots, X_k)$ and Y_{pred} were fitted as function of r for several distances from the central point. To find the maximum value of Y_{pred}, Lagrange's equation was used in agreement with Eq. (12).

$$(B - \mu.I).X = -\frac{b}{2} \tag{12}$$

The maximum or minimum values were obtained according to Eq. (13).

$$|B - \lambda.I| = 0 \tag{13}$$

A problem faced by the product development community is the selection of a set of conditions, which results in a product with a desirable combination of properties. This is essentially a problem involving the simultaneous optimization of several response variables (the desirable combination of properties), which depends upon a number of independent variables or sets of conditions. Derringer and Suich (1980) addressed this problem and presented a desirability function approach.

Suppose each of the k response variables is related to the p independent variables by Eq. (14).

$$Y_{ij} = f_i(X_1, X_2, X_3, \ldots, X_p) + \varepsilon_{ij}$$
$$i = 1, 2, \ldots, k \quad \text{and} \quad j = 1, 2, \ldots, n_i \tag{14}$$

Where f_i denotes the functional relationship between Y_i and $X_1, X_2, X_3, \ldots, X_p$. Note that this function may differ for each Y_i and that f_i represents this relationship except for an error term ε_{ij}. If we make the usual assumption that $(E(\varepsilon_{ij}) = 0)$ for each i, then we can relate the average or expected response η_i to the p independent variables by Eq. (15).

$$\eta_i = f_i(X_1, X_2, X_3, \ldots, X_p) \quad i = 1, 2, \ldots, k \tag{15}$$

In practice, f_i is typically unknown. The usual procedure is often (but not necessarily) to approximate f_i by a polynomial function. We then estimate η_i by $Y_{i,aj}$, the estimator obtained through regression techniques. The desirability function involves transformation of each estimated response variable $Y_{i,aj}$ to a desirability value d_i, where $0 \le d_i \le 1$. The value of d_i increases as the desirability of the corresponding response increases. The individual desirabilities are then combined using a geometric mean, which is represented by Eq. (16).

$$F = (d_1 \times d_2 \times \ldots d_k)^{1/k} \tag{16}$$

This single value of F gives the overall assessment of the desirability of the combined response levels. Clearly the range of F will fall in the interval [0,1] and F will increase as the balance of the properties becomes more favorable. F also has the property that if any $d_i = 0$ (that is, if one of the response variables is unacceptable), $F = 0$. It is for these reasons that the geometric mean, rather than some other function of the d_i's such as the arithmetic mean, was used. We shall consider the transformation given by Eq. (17).

$$d_i = \left\{ \begin{array}{l} \left[\dfrac{Y_{i,aj} - Y_{i,*}}{c_i - Y_{i,*}} \right]^s \quad Y_{i,*} \le Y_{i,aj} \le c_i \\ \left[\dfrac{Y_{i,aj} - Y_i^*}{c_i - Y_i^*} \right]^t \quad c_i < Y_{i,aj} \le Y_i^* \end{array} \right\} \tag{17}$$
$$d_i = \{0 \quad Y_{i,aj} < Y_{i,*} \text{ or } Y_{i,aj} > Y_i^*\}$$

In this situation, $Y_{i,*}$ is the minimum acceptable value of $Y_{i,aj}$ and Y_i^* is the maximum acceptable value. Values of $Y_{i,aj}$ outside these limits would make the entire product unacceptable. The value selected for c_i would be that value of $Y_{i,aj}$ which was most desirable and could be selected anywhere between $Y_{i,*}$ and Y_i^*. The values of s and t in the two-sided transformations are parameters selected by experiments.

Results and Discussion

The results obtained were analyzed from the fitted empirical equations according to Eqs. (18)–(21) for the enrichment of the fluid phase, the percentage of product recovery, the productivity and total cycle time, respectively.

$$E = 97.67 - 0.294.P_h - 1.294.P_l - 0.316.v + 0.392.T - 1.143.P_h^2 + 0.704.P_l^2 + 0.176.P_l.v \tag{18}$$

$$R = 67.481 - 0.56.P_h - 7.257.P_l + 4.483.v + 7.875.T + 8.994.P_h^2 + 0.747.P_l^2 + 0.245.v^2 + 1.572.T^2 + 1.275.P_h.P_l + 2.504.P_h.v + 0.47.P_h.T - 0.813.P_l.v + 0.611.P_l.T + 0.203.v.T \tag{19}$$

$$P = 5.126 + 0.151.P_h - 0.683.P_l + 3.321.v + 0.59.T + 0.848.P_h^2 - 0.0043.P_l^2 + 0.094.v^2 + 0.0821.T^2 + 0.0201.P_h.P_l - 0.295.P_h.v + 0.0033.P_h.T - 0.551.P_l.v + 0.0585.P_l.T + 0.391.v.T \tag{20}$$

$$t = 75.072 + 58.359.P_h - 3.998.P_l - 44.183.v - 4.274.T + 13.865.v^2 - 26.466.P_h.v + 3.594.P_l.v \tag{21}$$

Equations (22)–(25) were obtained in agreement with Eq. (12) for the enrichment of the fluid

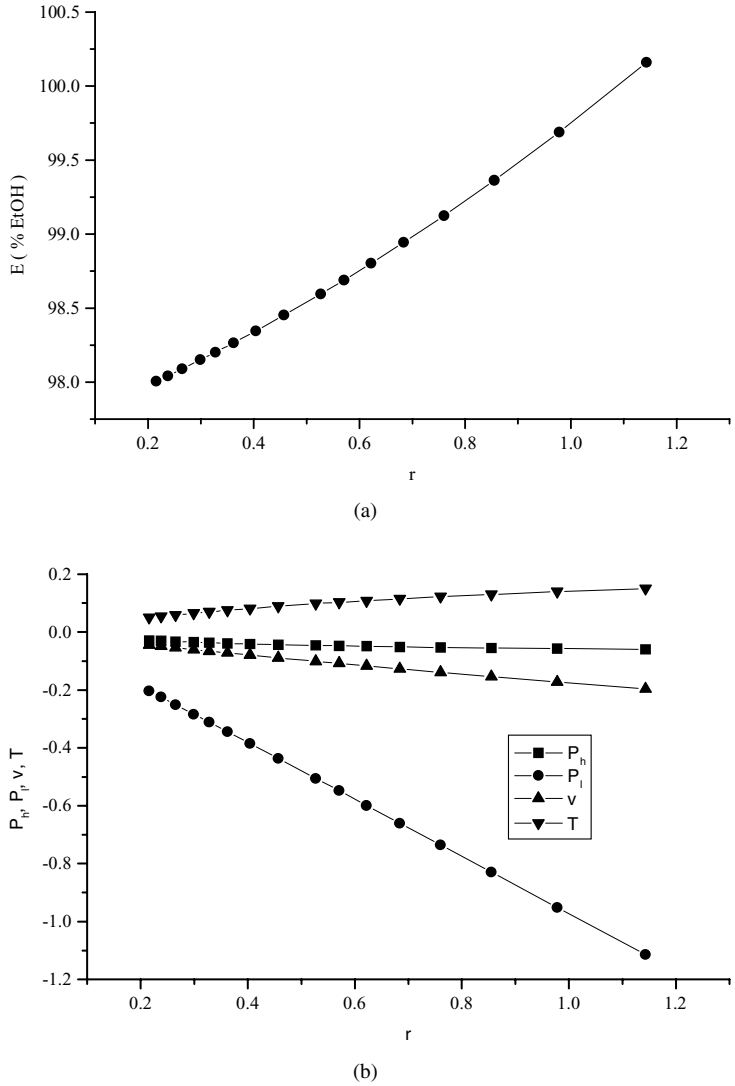

Figure 2. (a) Ridge analysis to the enrichment of the fluid phase (E versus r), (b) Ridge analysis to the enrichment of the fluid phase (variables versus r).

phase, recovery, productivity and total cycle time, respectively.

$$\begin{vmatrix} -1.14-\mu & 0 & 0 & 0 \\ 0 & 0.70-\mu & 0.08 & 0 \\ 0 & 0.08 & -\mu & 0 \\ 0 & 0 & 0 & -\mu \end{vmatrix} \begin{vmatrix} P_h \\ P_l \\ v \\ T \end{vmatrix} = \begin{vmatrix} 0.14 \\ 0.64 \\ 0.15 \\ -0.19 \end{vmatrix} \tag{22}$$

$$\begin{vmatrix} 8.99-\mu & 0.63 & 1.25 & 0.23 \\ 0.63 & 0.74-\mu & -0.40 & 0.30 \\ 1.25 & -0.40 & 0.24-\mu & 0.10 \\ 0.23 & 0.30 & 0.10 & 1.57-\mu \end{vmatrix} \begin{vmatrix} P_h \\ P_l \\ v \\ T \end{vmatrix} = \begin{vmatrix} 0.28 \\ 3.62 \\ -2.24 \\ -3.93 \end{vmatrix} \tag{23}$$

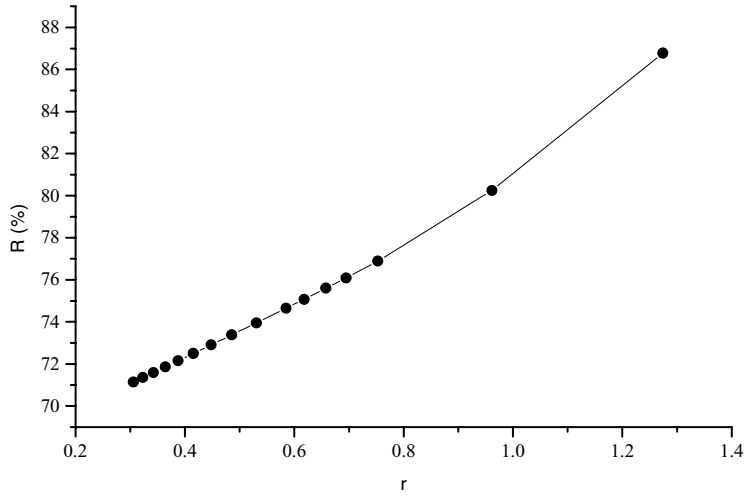

(a)

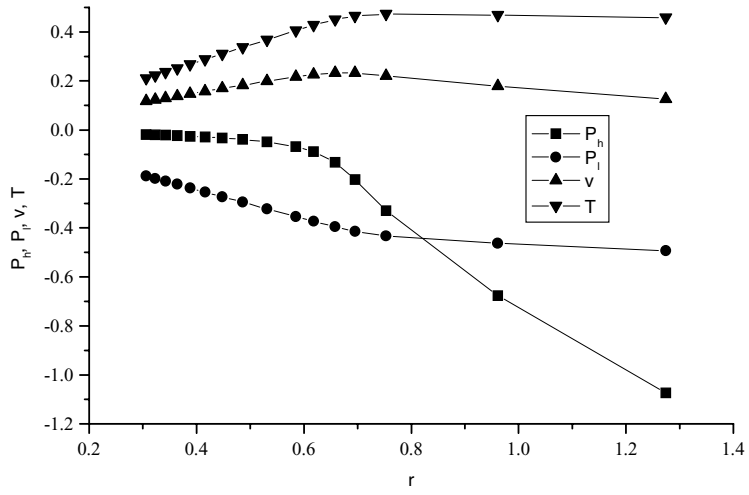

(b)

Figure 3. (a) Ridge analysis to the percentage of product recovery (R versus r), (b) Ridge analysis to the percentage of product recovery (variables versus r).

$$\begin{vmatrix} 0.84-\mu & 0.010 & -0.14 & 0.001 \\ 0.01 & -0.004-\mu & -0.27 & 0.029 \\ -0.14 & -0.27 & 0.09-\mu & 0.195 \\ 0.001 & 0.029 & 0.195 & 0.08-\mu \end{vmatrix} \begin{vmatrix} P_h \\ P_l \\ v \\ T \end{vmatrix} = \begin{vmatrix} -0.07 \\ 0.341 \\ -1.66 \\ -0.29 \end{vmatrix} \tag{24}$$

$$\begin{vmatrix} -\mu & 0 & -13.23 & 0 \\ 0 & -\mu & 1.597 & 0 \\ -13.23 & 1.59 & 13.86-\mu & 0 \\ 0 & 0 & 0 & -\mu \end{vmatrix} \begin{vmatrix} P_h \\ P_l \\ v \\ T \end{vmatrix} = \begin{vmatrix} -29.18 \\ 1.99 \\ 22.09 \\ 2.17 \end{vmatrix} \tag{25}$$

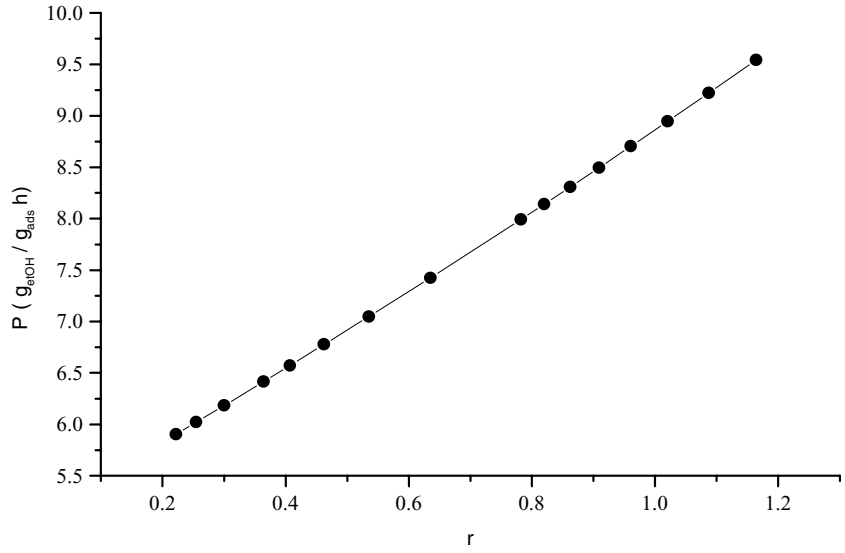

(a)

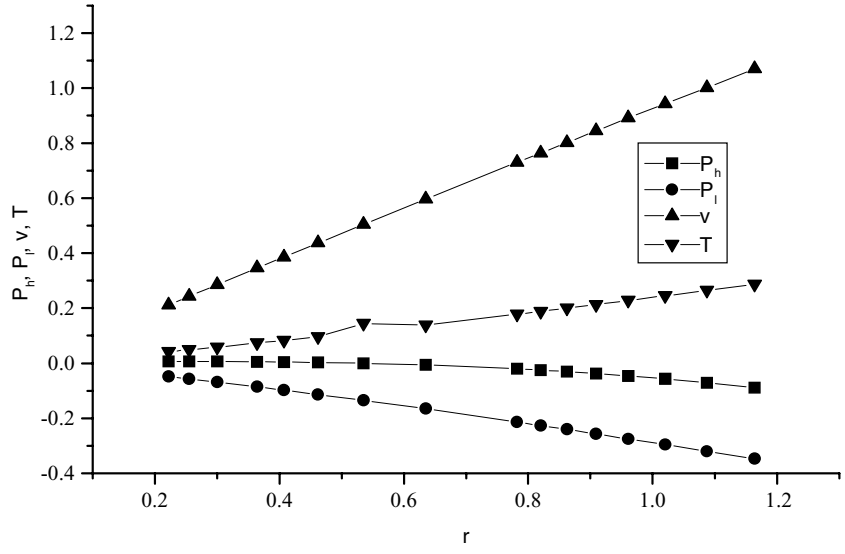

(b)

Figure 4. (a) Ridge analysis to the productivity (P versus r), (b) Ridge analysis to the productivity (variables versus r).

Equations (26)–(29) were obtained to relate the variables P_h, P_l, v and T, respectively, as a function of μ, in agreement with the solution of the Eq. (22) (enrichment of the fluid phase).

$$P_h = -\frac{147}{(1143 + 1000.\mu)} \tag{26}$$

$$P_l = -\frac{0.125.(80875.\mu + 1738)}{(-121 - 11000.\mu + 15625.\mu^2)} \tag{27}$$

$$v = -\frac{0.125.(19750.\mu - 6787)}{(-121 - 11000.\mu + 15625.\mu^2)} \tag{28}$$

$$T = \frac{0.196}{\mu} \tag{29}$$

Figure 2(a) and (b) show the results obtained for the enrichment for several values of μ bigger than 0.714 (value of the maximum solution of the Eq. (13)). The values of the variables were calculated through

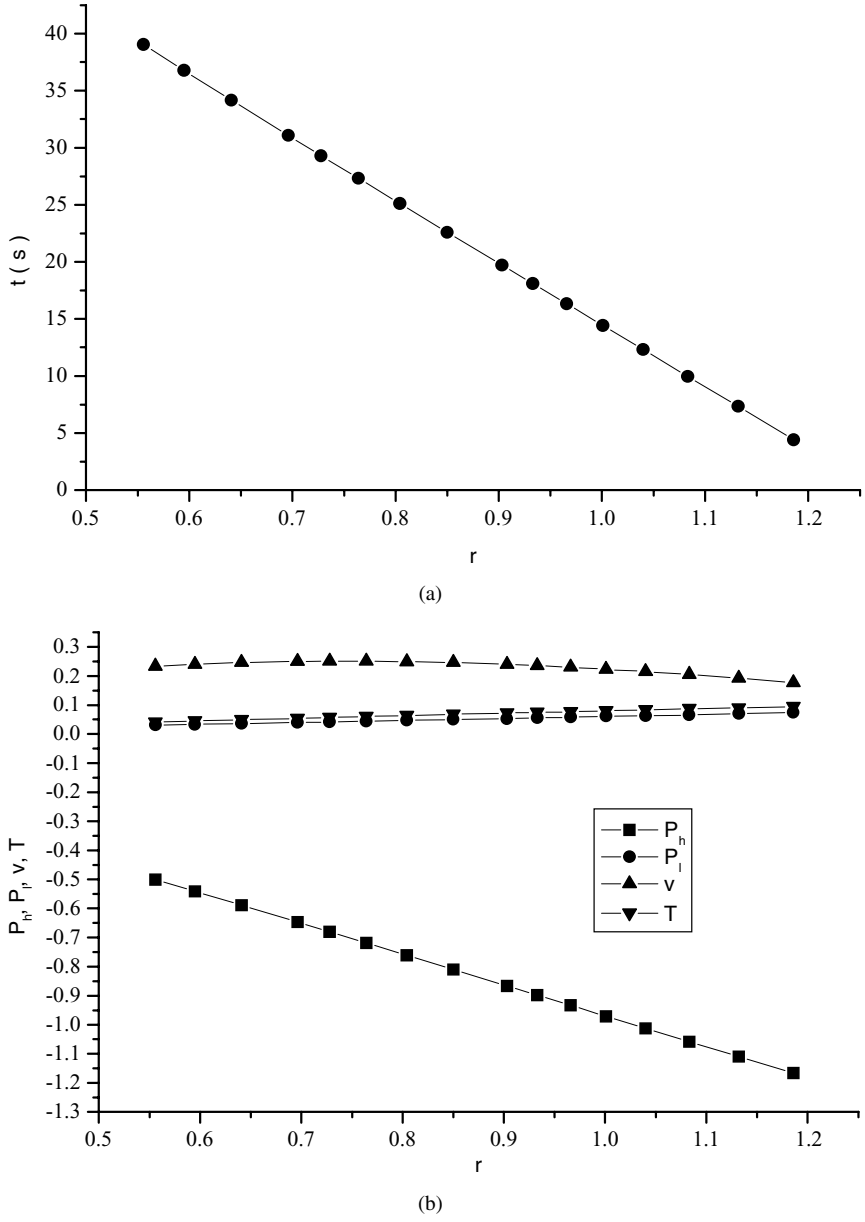

Figure 5. (a) Ridge analysis to the total time of the cycle (t versus r), (b) Ridge analysis to the total time of the cycle (variables versus r).

Eqs. (26)–(29). The values of the enrichment of the fluid phase were calculated through Eq. (18) and the values of r were calculated through Eq. (11). It can be observed that E increases as r increases. According to the limit of the experimental range, the maximum value of r is 1.06 and the values of the transformed variables are $P_h = -0.05$ (or 5.80 bar), $v = -0.175$ (or 4.47 l/h) and $T =, 0.15$ (or 207.5°C). The maximum value of the enrichment is 99.824%, in ethanol weight.

As done before, Fig. 3(a) and (b) show the results obtained for the recovery for several values of μ bigger than 9.218 (value of the maximum solution of the Eq. (13)). It can be observed that R increases as r increases. According to the limit of the experimental range, the maximum value of r is 1.20

and the values of the variables are $P_l = -0.475$ (or 0.35 bar), $v = -0.15$ (or 5.45 l/h) and $T = 0.45$ (or 222.5°C). The maximum value of the recovery is 85.150%.

As done before, Fig. 4(a) and (b) show the results obtained for the productivity for several values of μ bigger than 0.882 (value of the maximum solution of the Eq. (13)). It can be observed that P increases as $r$increases. According to the limit of the experimental range, the maximum value of r is 1.10 and the values of the variables are $P_h = -0.75$ (or 3 bar), $P_l = -0.325$ (or 0.4 bar) and $T = 0.25$ (or 212.5°C). The maximum value of the productivity is 9.822 $g_{ethanol}/g_{ads}h$.

Finally, Fig. 5(a) and (b) show the results obtained for the total cycle time for several values of μ smaller than -8.091 (value of the minimum solution of the Eq. (13)). It can be observed that t decreases as r increases. According to the limit of the experimental range, the maximum value of r is 1.025 and the values of the transformed variables are $P_l = 0.075$ (or 0.52 bar), $v = 0.212$ (or 5.63 l/h) and $T = 0.10$ (or 205.00°C). The minimum value of the total cycle time is 12.91 s.

The optimal combinations are in Tables 5–8,respectively, for the enrichment of the fluid phase, the percentage of product recovery, the productivity and total cycle time.

The individual desirabilities (d_i) were calculated through Eqs. (30)–(33) for the enrichment of the fluid phase, the percentage of product recovery, the productivity and total cycle time, respectively.

$$d_E = \left\{ \begin{array}{ll} \left[\dfrac{E-95}{99.99-95}\right]^1 & 95 \le E \le 99.99 \\ \left[\dfrac{E-100}{99.99-100}\right]^{0.1} & 99.99 < E \le 100 \end{array} \right\} \quad (30)$$

$$d_E = \{0 \quad E < 95 \text{ or } E > 100\}$$

$$d_R = \left\{ \begin{array}{ll} \left[\dfrac{R-0}{99.99-0}\right]^1 & 0 \le R \le 99.99 \\ \left[\dfrac{R-100}{99.99-100}\right]^{0.1} & 99.99 < R \le 100 \end{array} \right\} \quad (31)$$

$$d_R = \{0 \quad R < 0 \text{ or } R > 100\}$$

$$d_P = \left\{ \begin{array}{ll} \left[\dfrac{P-0}{9.99-0}\right]^1 & 0 \le P \le 9.99 \\ \left[\dfrac{P-10}{9.99-10}\right]^{0.1} & 9.99 < P \le 10 \end{array} \right\} \quad (32)$$

Table 5. Optimal combination for enrichment of the fluid phase.

P_h (bar)	P_l (bar)	v (l/h)	T (°C)	E (% in ethanol weight)
5.80	0.20	4.47	207.50	99.824

Table 6. Optimal combination for product recovery.

P_h (bar)	P_l (bar)	v (l/h)	T (°C)	R (%)
2.00	0.35	5.45	222.50	85.150

Table 7. Optimal combination for productivity.

P_h (bar)	P_l (bar)	v (l/h)	T (°C)	P ($g_{ethanol}/g_{ads}h$)
3.00	0.40	8.00	212.50	9.822

Table 8. Optimal combination for the total time of the cycle.

P_h (bar)	P_l (bar)	v (l/h)	T (°C)	t (s)
2.00	0.52	5.63	205.00	12.910

$$d_P = \{0 \quad P < 0 \text{ or } P > 10\}$$

$$d_t = \left\{ \begin{array}{ll} \left[\dfrac{t-0}{1-0}\right]^{0.1} & 0 \le t \le 1 \\ \left[\dfrac{t-240}{0-240}\right]^1 & 0 < t \le 240 \end{array} \right\} \quad (33)$$

$$d_t = \{0 \quad t < 0 \text{or } t > 240\}$$

An analytical solution was developed through MATLAB program. The optimal values of the variables are summarized in Table 9.

An increase in the flow rate led to a decrease in the enrichment of the product, for all the operation pressures analyzed. This happened due to a shorter retention time of the mixture ethanol-water in contact with the adsorbent bed for the larger flow rates, which caused a decrease in the amount of adsorbed water, at the same operation pressure. On the other hand, an increase in the adsorption pressure led to an increase in enrichment for all flow rates, yielding pure ethanol (99.999%) for a pressure of 6 bar and a flow rate of 2 l/h.

This fact comes to meet the theory of the PSA process, where the adsorption step occurs at high pressures, favoring the uptake of water by the increase of its partial pressure, and the desorption step occurs at low pressures, by the fast decrease of the

Table 9. Optimal values of the variables.

P_h (bar)	P_l (bar)	v (l/h)	T (°C)	E (% in ethanol weight)	R (%)	P ($g_{ethanol}/g_{ads}h$)	t (s)
3.397	0.20	5.52	250.00	99.683	89.693	7.462	28.98

partial pressure of the more strongly adsorbed component. With respect to the percentage of product recovery, it was observed that an increase in the flow rate, at a given fixed adsorption pressure, caused an increase in this percentage, a value of 90% being reached for a flow rate of 8 l/h and an adsorption pressure of 2 bar. In contrast, an increase in the pressure reduced this recovery, for all the flow rates adopted.

The productivity had a similar behavior as the percentage of recovery of the product. In other words, a flow rate increase produced a larger quantity of purified product, per unit of adsorbent mass per unit of total cycle time, at a given fixed adsorption pressure.

Table 10. Preliminary results for enrichment of the fluid phase.

Run	T (°C)	P_h (bar)	v (l/h)	P_l (bar)	E (% in ethanol weight)
1	200	2	2	0.2	98.813
2	200	2	4	0.2	98.264
3	200	2	6	0.2	97.903
4	200	2	8	0.2	97.796
5	200	4	2	0.2	99.630
6	200	4	4	0.2	98.990
7	200	4	6	0.2	98.500
8	200	4	8	0.2	98.300
9	200	6	2	0.2	99.735
10	200	6	4	0.2	99.074
11	200	6	6	0.2	98.603
12	200	6	8	0.2	98.396

Table 11. Preliminary results for product recovery.

Run	T (°C)	P_h (bar)	v (l/h)	P_l (bar)	R (%)
1	200	2	2	0.2	82.12
2	200	2	4	0.2	85.31
3	200	2	6	0.2	87.21
4	200	2	8	0.2	90.06
5	200	4	2	0.2	73.80
6	200	4	4	0.2	77.35
7	200	4	6	0.2	80.04
8	200	4	8	0.2	83.70
9	200	6	2	0.2	70.11
10	200	6	4	0.2	74.25
11	200	6	6	0.2	77.63
12	200	6	8	0.2	82.03

Table 12. Preliminary results for productivity.

Run	T (°C)	P_h (bar)	v (l/h)	P_l (bar)	P ($g_{et}/g_{ads}h$)
1	200	2	2	0.2	2.464
2	200	2	4	0.2	5.091
3	200	2	6	0.2	7.868
4	200	2	8	0.2	10.779
5	200	4	2	0.2	2.213
6	200	4	4	0.2	4.618
7	200	4	6	0.2	7.218
8	200	4	8	0.2	10.019
9	200	6	2	0.2	2.103
10	200	6	4	0.2	4.433
11	200	6	6	0.2	7.001
12	200	6	8	0.2	9.819

Table 13. Preliminary results for the total time of the cycle.

Run	T (°C)	P_h (bar)	v (l/h)	P_l (bar)	t (s)
1	200	2	2	0.2	50.02
2	200	2	4	0.2	30.11
3	200	2	6	0.2	20.17
4	200	2	8	0.2	15.04
5	200	4	2	0.2	99.97
6	200	4	4	0.2	60.18
7	200	4	6	0.2	46.09
8	200	4	8	0.2	30.21
9	200	6	2	0.2	150.07
10	200	6	4	0.2	90.23
11	200	6	6	0.2	70.02
12	200	6	8	0.2	50.06

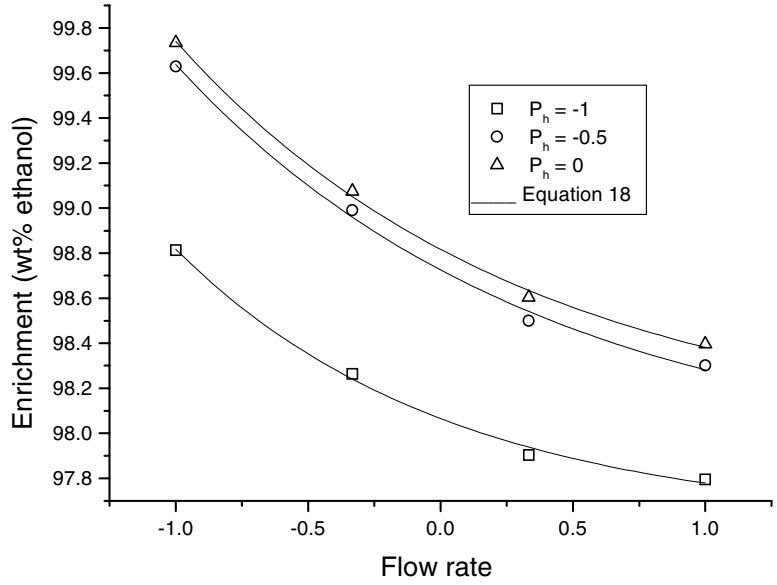

Figure 6. Empirical model for enrichment of the fluid phase.

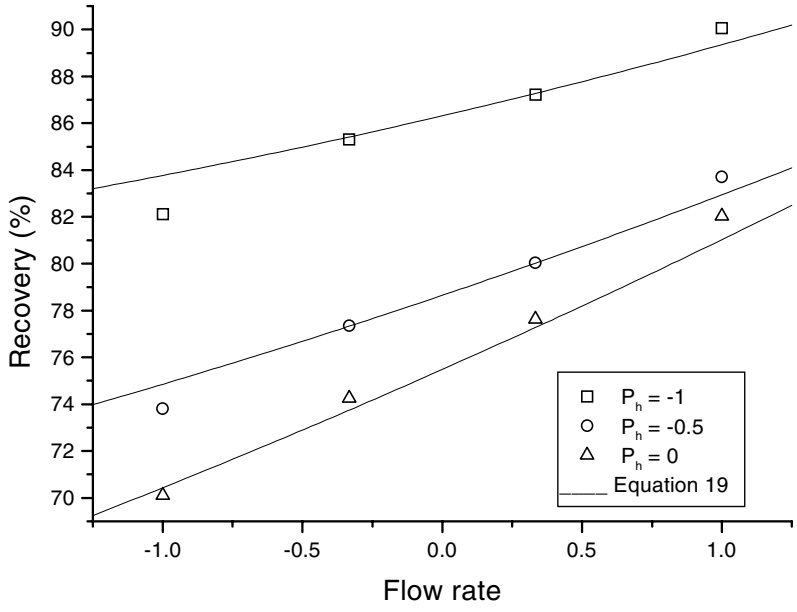

Figure 7. Empirical model for product recovery.

An increase in the adsorption pressure, at a given fixed flow rate, reduced the productivity. These facts can be explained by the increase in the total cycle time for these analyzed conditions.

The preliminary results are in Tables 10–13 for the enrichment of the fluid phase, product recovery, the productivity, and the total cycle time, respectively.

The preliminary results were compared with the empirical models in Figs. 6–9 for the enrichment, the recovery, the productivity and total cycle time, respectively.

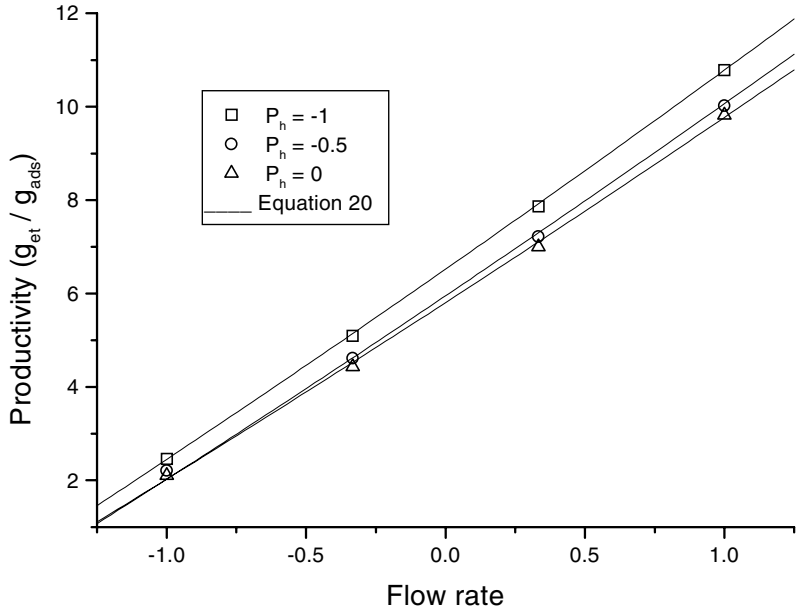

Figure 8. Empirical model for the productivity.

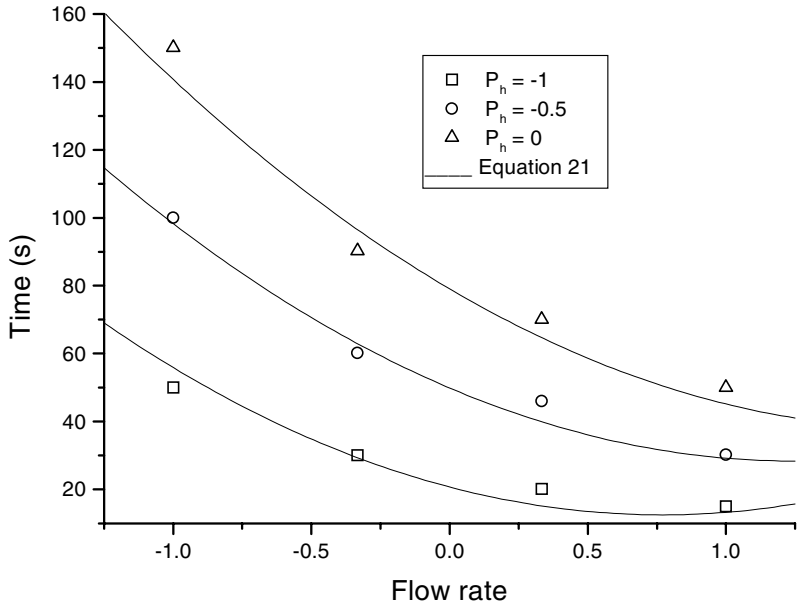

Figure 9. Empirical model for the total time of the cycle.

Conclusions

A PSA system was shown to be successful and versatile for the collection of experimental data for ethanol-water separation. Pure ethanol was obtained under certain operating conditions, and there was a consistency among the findings of interest. The adopted variables influenced the obtained results. An increase in the flow rate caused a decrease in the quality of the product (enrichment of the ethanol). At the same time, it provided an increase in its recovery and productivity. On the other hand, increasing pressure led to an improvement

in the enrichment, but a decrease in the recovery and the productivity. The empirical models were shown to be satisfactory. The ridge analysis method and the multi-response method were effective for the determination the optimal variable responses.

Nomenclature

A_{cs} Area of the bed (cm^2)
E Enrichment of the product (% in ethanol weight)
H_{cs} Height of the bed (cm)
M_f Product mass in the recipient R1, for operation cycle (g)
M_o Mass of feeding fluid (g)
M_s Mass of activated adsorbent (g)
P Productivity ($g_{ethanol}/g_{ads}h$)
P_h Adsorption pressure (bar)
P_l Desorption pressure (bar)
R Percentage of ethanol recovery (%)
t Total time of the cycle (s)
t_d Time of discharge (s)
t_{pr} Time of pressurization (s)
t_v Desorption time (s)
V_{cs} Volume of the bed (cm^3)
X_f Concentration of the product in the recipient R1, at steady-state (% in ethanol weight)
X_o Concentration of the feeding fluid (% in ethanol weight)
ϕ_{cs} Diameter of bed (cm)
ε_L Porosity of the bed
ρ_b Packing density of the bed (g/cm^3)
ρ_p Apparent density of the adsorbent (g/ml)
ρ_L Density of the feeding fluid (g/ml)
ν Flow rate (l/h)

References

Azevedo, D.C.S., "Estudo Cinético e Termodinâmico da Adsorção para o Sistema Etanol-Água sobre Zeólita 3A," Dissertação, Universidade Federal de São Carlos, p. 195, 1992.

Carmo, M.J. and J.C. Gubulin, "Ethanol-Water Adsorption on Commercial 3A Zeolites: Kinetic and Thermodynamic Data," *Brazilian Journal of Chemical Engineering*, **14**(3), 217–224 (1997).

Carton, A. et al., "Separation of Ethanol-Water Mixtures Using 3A Molecular Sieve," *J. Chem. Tech. Biotechnol.*, **39**, 125–132 (1987).

Cassidy, R.T. and E.S. Holmes, "Twenty-Five Years of Progress in Adiabatic Process," *A.I.Ch.E. Symp. Ser.*, **80**, 68–75, 223 (1984).

Keller, G.E., "Gas Adsorption Process: State of Art in Industrial Gas Separations," *Am. Chem. Soc. Symp. Ser.*, **223**, 145–149 (1983).

Mersmann, A. et al., "Separation of Gas Mixtures by Adsorption," *Ger. Chem. Engng.*, **7**, 137–149 (1984).

Skarstrom, C.W., "Use of Adsorption Phenomena in Automatic Plant-Type Gas Analysers," *Ann. N.Y. Acad. Sci.*, **72**, 751–763 (1959).

Sowerby, B. and B.D. Crittenden, "Scale-up of Vapour Phase Adsorption Columms for Breaking Ethanol-Water Azeotrope," *I. Chem. E. Symp. Ser.*, **118** (1991).

Teo, W.K. and D.M. Ruthven, "Adsorption of Water from Aqueous Ethanol Using 3A Molecular Sieves," *Ind. Eng. Chem. Proc. Des. Dev.*, **25**(1), 17–21 (1986).